

# Numerical Simulation Study on Co-combustion Characteristics of Biogas and Antibiotic Filter Residue in a Grate Furnace

Xinyue Gao, Chang'an Wang\*, Chengchang Liu, Gaofeng Fan, Qisen Mao, Defu Che

State Key Laboratory of Multiphase Flow in Power Engineering, School of Energy and Power Engineering, Xi'an Jiaotong University, Xi'an 710049, China

\*corresponding author, email: changanwang@mail.xjtu.edu.cn

## ABSTRACT

The treatment of antibiotic filter residue (AFR) is an important issue, because of its special nature, the large output, and the difficulty of combustion. Nowadays, the AFR is generally incinerated, but dioxins are produced during the process, which makes incineration technology face challenges. There is a lack of research on the influences of co-combustion conditions on temperature field and flue gas characteristics, but it plays an important role in practical applications. The present study aimed to investigate the influences of AFR mixed with biogas on furnace temperature field and emission characteristics through numerical simulation. The results showed that the opposed injection position was the best type when the proportion of mixed biogas was constant. The results can provide new insight into co-combustion and thermal utilization of AFR.

**Keywords:** biomass fuel, co-combustion, numerical simulation, antibiotic filter residue, grate furnace

## NONMENCLATURE

### Abbreviations

AFR	Antibiotic filter residue
PS	Peanut shell
PL	Poplar

## 1. INTRODUCTION

With the fast development of the medical industry, the output of medical drugs and antibiotic filter residue (AFR) have rapidly increased. Most of the antibiotics are produced by biological fermentation technology [1].

Simultaneously, millions of tons of AFR have been generated during this process [2]. The antibiotics in China account for more than 70% of the world's total production, while the residue amount is growing at a rate of about 10% per year [3]. Due to the limitation of the extraction method, there inevitably remains a few antibiotics in the residue. Therefore, AFR unavoidably causes environmental pollutions without harmless disposal [4, 5]. But AFR is also one of the typical biomass resources, with the potential for efficient small-scale utilization.

Methods to achieve clean and safe treatment of AFR includes combustion, anaerobic digestion, pyrolysis, and hydrothermal treatment, etc. Co-combustion is an effective approach to improve fuel flexibility and combustion performance. Yang et al. [6] explored the combustion characteristics of AFR and observed three main stages of the combustion process. Zhang et al. [7] investigated the effect of water vapor addition during AFR combustion. Nevertheless, the previous studies on the AFR primarily concentrated on the thermochemical transformation and the conversion of low-grade energy fuel to high-quality energy fuel, while the influences of co-combustion condition on the temperature field and the flue gas characteristics are still unclear. The injection location, mixing ratio, and composition of biogas are the important conditions for co-combustion.

The present study dealt with the combustion temperature field and the characteristics of the flue gas under different blending conditions. The peanut shell (PS)-AFR and poplar (PL)-AFR were burned in a heating biomass chain furnace, respectively. In addition, a certain amount of biogas was injected to increase the combustion temperature within the furnace. The research mainly studied the influence of the position of

Selection and peer-review under responsibility of the scientific committee of the 12th Int. Conf. on Applied Energy (ICAE2020).

Copyright © 2020 ICAE

the biogas injection, and provided new insight into co-combustion and thermal utilization of AFR through numerical simulation.

## 2. MATERIAL AND METHODS

The combustion process in the furnace is simplified into a gas phase combustion process reasonably in the numerical simulation modeling, and the tiny particles suspended in the furnace can be converted into the combustible gas in the furnace by a thermal calculation.

### 2.1 Geometric model and meshing

The boiler was divided into the geometry model by a structured grid. The sub-blocks included the area under the furnace arch, the furnace throat, and the furnace upper. The intensive combustion burner area had meshed, as shown in Fig 1a.

The calculation area was the inside of the furnace where the upper part of the grate was the boundary of the co-combustion fuel inlet. According to the different components of the flue gas entering the furnace at different positions on the grate, the grate was divided into 8 smaller grate units. The changes in the inlet parameters of the grate unit were used to simulate the composition of the flue gas at different positions in the actual combustion process. The layout of each entrance boundary is shown in Fig 1b.

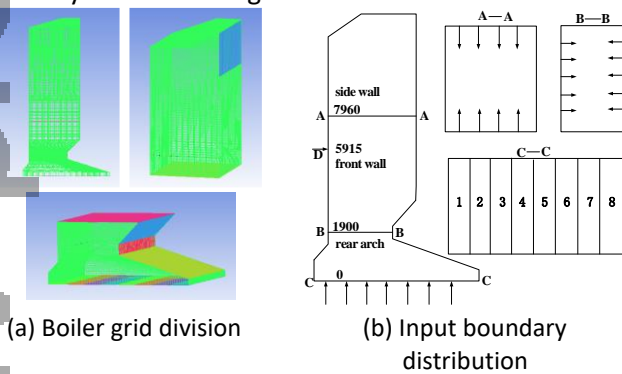


Fig 1 Modeling schematic diagram

### 2.2 Boundary conditions

The analysis results of samples used in the simulation are shown in Table 1 and Table 2. The excess air coefficient was 1.35, the primary air accounted for 80% of the total air volume, and the secondary air accounted for 20% of the total air volume. The primary and secondary air temperatures were set to 126 °C. The amount of air required for combustion was calculated by the amount of fuel, and then the size of the nozzle was determined by the wind speed of the secondary air outlet.

Pyrolysis occurred first after heating when the fuel was fed into the furnace, a large amount of combustible gas was produced at the front of the grate. Subsequently, the pyrolyzed fuel had undergone a combustion reaction on the grate under continuous heating, and the temperature in the middle and rear parts of the grate was the highest. The specific distributions are shown in Fig 2 and Fig 3.

Table 1. Proximate analysis of experimental

Samples	$Q_{net,ar}$	Proximate analysis/%			
		$M_t$	$A_{ar}$	$V_{ar}$	$FC_{ar}$
PS	13.79	10.9	7.15	63.75	18.20
PL	17.81	2.5	0.59	82.07	14.85
AFR	12.78	19.0	12.75	61.32	6.93

Table 2. Ultimate analysis of experimental

Samples	Ultimate analysis/%				
	$C_{ar}$	$H_{ar}$	$N_{ar}$	$O_{ar}$	$S_{ar}$
PS	38.34	4.34	1.08	29.47	0
PL	47.04	6.38	0.28	43.17	0.039
AFR	32.0	3.23	5.11	27.48	0.43

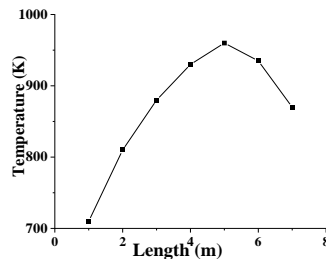


Fig 2 Grate temperature distribution

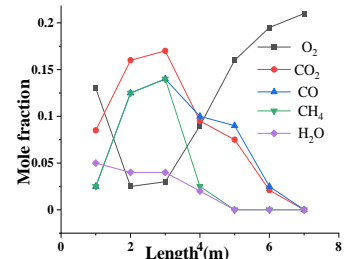


Fig 3 Input gas concentration distribution in the grate

## 3. RESULTS AND DISCUSSION

The present research involved the influences of the proportion of blended biogas, the spraying position, and the change of biogas composition. The following is a specific study on the impact of biogas injection position.

### 3.1 Model validation

In this section, based on the design parameters in Section 2.2, the accuracy of the model was verified by comparing the design parameters with the flue gas temperatures at the furnace outlet according to simulation results. The simulation resulted that the model calculation error was within the allowable range.

### 3.2 The influence of the biogas injection position

The mixed combustion ratio of peanut shell (PS)-antibiotic filter residue (AFR) and poplar (PL)-AFR were determined to be 1:1 by mass, and the ratio of mixed biogas was 20%. The spraying positions were front wall injection, opposed injection, and rear arch injection.

As shown in Fig 4, when the combustion of biomass pyrolysis gas begins, the furnace temperature rises below 8 m in the furnace. The area below the height of the rear arch is the reaction zone. The average temperature of the furnace cross-section rises faster. It is sprayed at the height of the arch and continues to burn after mixing with air. The average temperature of the furnace section slow rises. The secondary air is fed into the middle of the furnace, which causes the average temperature of the middle section to decrease. The biogas burns quickly, and it burns completely after being sprayed into the furnace. After the front wall and side walls are sprayed with secondary air, the average temperature of the basic section of the upper part of the furnace is almost unchanged, thus, the high-temperature zone of the furnace is mainly in the rear arch between and the middle of the furnace. With the injection of secondary air, the O<sub>2</sub> concentration along the height of the furnace changes three times.

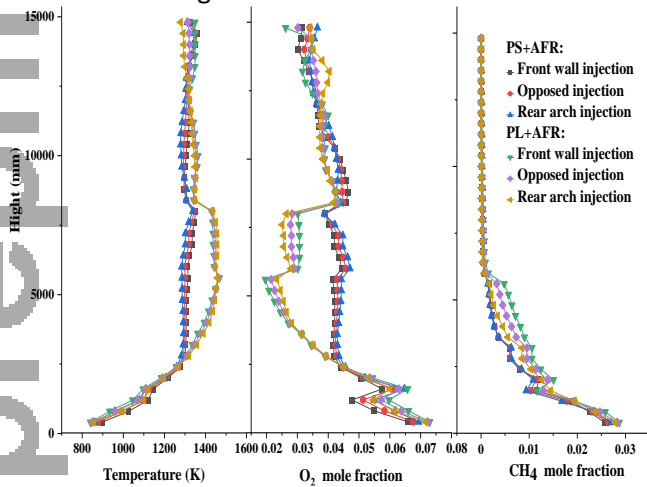


Fig 4 The variation of average cross-section temperature, O<sub>2</sub> concentration, and CH<sub>4</sub> concentration along with the height of the furnace under different injection locations

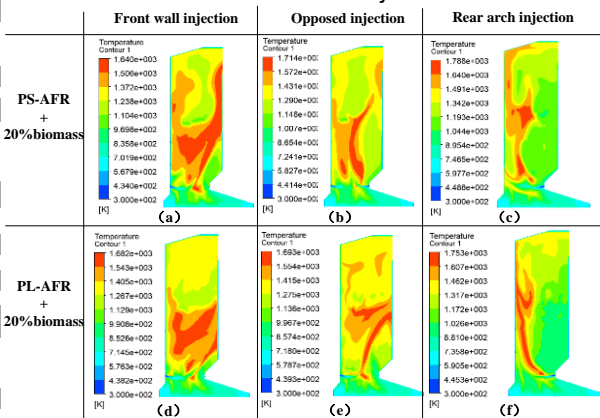


Fig 5 Average temperature of furnace center section at different injection positions

It can be seen from Fig 5 that the mixed biogas is sprayed from the front wall, and the flame in the furnace

moves to the back wall. This is because the sprayed biogas passes through the flue gas from the grate, and part of it reaches the back wall and burns. The pressure at the upper rear wall is low, so the biogas reaching the rear wall burns near the wall, causing the flame to elongate and causing the temperature of the rear wall to rise.

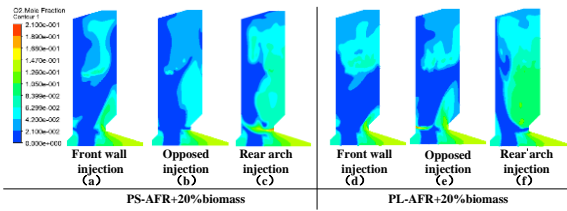


Fig 6 O<sub>2</sub> concentration distribution in the central section of the furnace at different injection positions

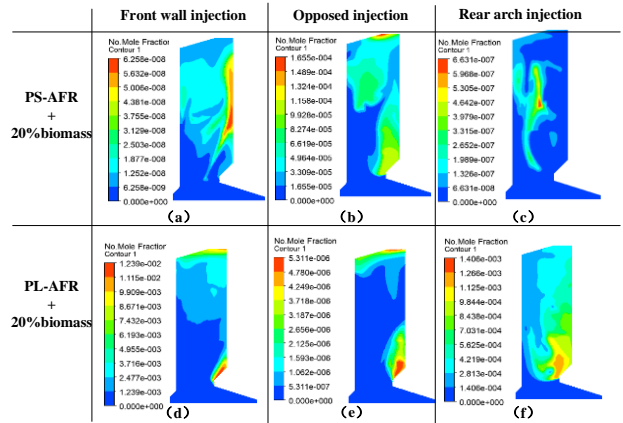


Fig 7 Distribution of NO concentration in the central section of the furnace at different injection positions

As shown in Fig 6 and Fig 7, from the rear arch to the middle of the furnace is the main combustion area of pyrolysis gas and mixed biogas. Therefore, the O<sub>2</sub> concentration in this area is low. The injection of secondary air on the side wall causes the O<sub>2</sub> concentration in the upper part of the furnace to increase. A "Y"-shaped O<sub>2</sub> concentration distribution field is formed inside the furnace. Moreover, an oxygen-rich area is formed above the rear arch. There is a fuel-rich zone at the bottom of the furnace, where the reducibility is high, and there is basically no generation of NO. In the combustion zone above the furnace throat, the fuel-rich zone contains less NO. The generation of NO mainly occurs in two areas, one in the upper part of the furnace. In this area, the injected biogas and pyrolysis gas basically achieve complete combustion. The flue gas temperature is high. In addition, due to the influence of the secondary air injection on the side wall, the O<sub>2</sub> concentration in the upper part of the furnace rises and is at a high temperature. An oxygen-rich environment is conducive to the production of NO. The oxygen-rich area formed above the rear arch is also the main area for NO

generation. Due to the rear arch structure, the flue gas input from the grate is guided by the front wall, and a low-pressure area is formed above the rear arch, which can be introduced from the discharged oxygen-rich flue gas in the furnace. Besides, the height of this area is a local high-temperature zone where the combustion reaction of the mixed biogas occurs. Hence, a high-temperature oxygen-rich environment is also formed here, which is conducive to the generation of NO.

In conclusion, the maximum local temperature in the furnace is higher with the opposed injection method than with the front wall injection method. Because the injected biogas and air are more fully mixed with the opposed injection method, and the combustion is more intense, and the CH<sub>4</sub> concentration at the outlet of the furnace is the lowest, indicating that the combustion efficiency of biogas is the highest in the opposed combustion mode. Judging from the average temperature of the flue gas at the furnace outlet, the total amount of combustible gas in the biogas input is constant, and the heat generated is constant. There is no significant difference between the three injection positions and the smoke at the furnace outlet.

#### 4. CONCLUSIONS

This paper researches the influence of the biogas injection position on the temperature field within the furnace and the flue gas characteristics through numerical simulation. It is recommended to use opposed injection when the mixed combustion ratio of peanut shell to antibiotic filter residue and the ratio of poplar to antibiotic filter residue is determined to be 1:1 by mass and the ratio of mixed combustion of biogas is 20%. For the front wall injection position, the injection speed of the front wall injection increases with the increase of the proportion of mixing, the biogas passing through the flue gas of the furnace and burning near the back wall. As a result, the temperature of the back wall is too high, which affects the working performance of the back water wall and the temperature distribution within the furnace. Similarly, the rear arch injection position also leads to the combustion of biogas near the front wall. The front water wall in a high-temperature environment, and the furnace flame to be less full. During the opposed injection positions, the combustion process of biogas is mainly in the middle of the furnace, the temperature is evenly distributed, and the combustion flame is fuller.

#### ACKNOWLEDGEMENT

The authors acknowledged the financial support from the China Postdoctoral Science Foundation

(2019T120286) and the Natural Science Basic Research Plan in Shaanxi Province of China (2019JM-067).

#### REFERENCE

- [1] Wang P, Liu HL, Fu H, Cheng XW, Wang B, Cheng QH, et al. Characterization and mechanism analysis of penicillin G biodegradation with klebsiella pneumoniae Z1 isolated from waste penicillin bacterial residue. *Journal of Industrial and Engineering Chemistry*. 2015, 27:50-8.
- [2] Han HJ, Zheng SY, Ma WC, Huang JH, Chen LY, Liu X, et al. The current situation and treatment and disposal techniques of antibiotic bacterial residues in China. *Applied Mechanics and Materials*. 2014, 587-589:820-3.
- [3] Ma DC, Zhang GY, Zhao PT, Areeprasert C, Shen YF, Yoshikawa K, et al. Hydrothermal treatment of antibiotic mycelial dreg: More understanding from fuel characteristics. *Chemical Engineering Journal*. 2015, 273:147-55.
- [4] Ma D, Zhang G, Areeprasert C, Li C, Shen Y, Yoshikawa K, et al. Characterization of NO emission in combustion of hydrothermally treated antibiotic mycelial residue. *Chemical Engineering Journal*. 2016, 284:708-15.
- [5] Angeles LF, Islam S, Aldstadt J, Saqeeb KN, Alam M, Khan MA, et al. Retrospective suspect screening reveals previously ignored antibiotics, antifungal compounds, and metabolites in Bangladesh surface waters. *Science of the Total Environment*. 2020, 712.
- [6] Yang S, Zhu X, Wang J, Jin X, Liu Y, Qian F, et al. Combustion of hazardous biological waste derived from the fermentation of antibiotics using TG-FTIR and Py-GC/MS techniques. *Bioresource Technology*. 2015, 193:156-63.
- [7] Zhang G, Liu H, Ge Y, Gao S. Gaseous emission and ash characteristics from combustion of high ash content antibiotic mycelial residue in fluidized bed and the impact of additional water vapor. *Fuel*. 2017, 202:66-77.